Northumbria Research Link

Northumbria University
NEWCASTLE

University Library

Elemental Depth Profiling of Thin Film Chalcogenides Using MeV Ion Beam Analysis

Chris Jeynes[1*], Guillaume Zoppi[2], Ian Forbes[2], Melanie J. Bailey[1], Nianhua Peng[1*]

[1]University of Surrey Ion Beam Centre, Guildford GU2 7XH, UK
[2]Northumbria Photovoltaics Applications Centre, Northumbria University, Newcastle upon Tyne, NE1 8ST, UK
[*]Corresponding authors

Abstract: The comprehensive characterisation is one of many technical challenges in the fabrication of photovoltaic devices from novel materials. We show how the application of recent advances in MeV ion beam analysis, providing the self-consistent treatment of Rutherford backscattering and particle induced X-ray emission spectra, makes a new set of powerful complementary elemental depth profiling techniques available for all thin film technologies, including the chalcopyrite compound semiconductors. We will give and discuss a detailed analysis of a CuInAl metallic precursor film, showing how similar methods are also applicable to other films of interest.

I. INTRODUCTION

Chalcopyrite-based $CuIn_{1-x}Ga_xSe_2$ (CIGS) and $CuIn_{1-x}Al_xSe_2$ (CIAS) solar cells have achieved the highest level of performance to date for single junction polycrystalline thin film technology [1-3]. Interestingly, the high performance devices were fabricated with materials of a relatively low bandgap (E_g ~ 1.2 eV for 30% Ga or 13% Al substitution respectively). The poor device performance with higher bandgap materials is found to be associated with increased defect density and stronger interfacial recombination when the Ga or Al doping level is increased.

These materials are complex, and can be troublesome to fabricate, with many possible fabrication routes. While the most efficient devices so far have been deposited using the co-evaporation method, we have investigated the production of CIAS thin films by a two-stage process: the sputter deposition of Cu/In/Al (CIA) metallic precursor layers followed by annealing in a selenium environment to synthesize the compound [4]. In principle this method promises improved scalability for commercial production compared to other deposition methods, but on the other hand the selenisation technique can yield unwanted elemental depth profiles due to the binary selenides having different reaction temperatures. So that characterization methods are important for establishing the processes. As a part of our ongoing effort for in-depth analysis of CIA metallic precursors and CIGS and CIAS thin films, we will describe very novel methods of accurate thin film depth profiling using a self-consistent analysis of simultaneously collected spectra from MeV ion backscattering together with the stimulated photon emission from a typical CIA precursor film.

II. DEPTH PROFILING USING ION BEAM ANALYSIS

Conventional thin film depth profiling techniques such as Auger electron or X-ray photo-electron spectroscopy, or SIMS (secondary ion mass spectrometry) are plagued by artefacts including those of interfaces, and SIMS is not quantitative because of the large matrix effects. Other analytical methods such as SEM-EDS (energy dispersive X-ray spectrometry on the scanning electron microscope) have little or no depth resolution and do not work well for these thin films.

However, Rutherford backscattering (RBS) is a well-established non-destructive depth profiling technique [5] where the depth resolution comes from the energy loss of the probing beam (such as 1.5MeV $^4He^+$) detected after elastic scattering at backward angles from the atomic nuclei of the target; films of CIGS or CIAS of submicron thickness have very convenient energy loss of the primary beam with good depth resolution. Because the RBS elastic scattering cross-section is derived simply from the Coulomb potential [6], and the energy losses of light ion beams in materials are well known [7-9], RBS is an accurate technique suitable for standards work [10-11]. Depth profiles can now be extracted efficiently from RBS spectra (or other related particle scattering spectra) with computer codes validated by an IAEA-sponsored intercomparison exercise [12], including the DataFur-

nace code [13] used here.

On the other hand, RBS using MeV ion beams does not have good mass resolution for these chalcogenide compounds, and RBS also has low sensitivity for light elements in a heavy matrix (such as the Al in CuInAl) since the yield goes with Z^2.

Compared to SEM-EDS, particle-induced X-ray emission (PIXE) has orders of magnitude better sensitivity since there is effectively no bremsstrahlung from the primary beam, although it has a similarly poor depth resolution. However, the self-consistent analysis of RBS/PIXE data has recently been introduced, where the resulting analysis has the mass-sensitivity of PIXE combined with the depth-sensitivity of RBS [14-18]. We apply these methods here for the first time to complex thin film PV materials (but see [19]).

III. ANALYSIS

A CuInAl precursor film of about ⅓ μm was sputter deposited on a soda-lime glass substrate coated with a ¾ μm Mo electrode layer (sample N109G). The unheated substrates are rotated above the high purity targets to produce a structure of several hundred layers. The CIA film had a Cu seed and an In cap, both ~7nm thick. The PV absorber layer is subsequently made from this precursor film by selenisation of the CIA film in a tube furnace in Ar atmosphere and with vaporized selenium from a solid source.

The ion beam analysis was carried out on the 2MV Tandetron accelerator at Surrey [20] using 1.5MeV ^{4}He$^+$, two particle detectors with solid angles of 1.2msr and 6.4msr at scattering angles of 172° and 148° for RBS, and for PIXE a 3mm thick Si(Li) crystal with solid angle of 0.25msr at a backward angle to the beam of 60°, with an 8μm Kapton filter to stop backscattered particles.

The ^{4}He$^+$ beam current was ~30nA into a nominally 1mm diameter beam spot giving a counting rate of 33kHz in the large particle detector, but only 500Hz in the X-ray detector since the He-PIXE cross-sections are low. The particle detectors have pulse shaping amplifiers implementing pulse pileup rejection with a time resolution of about 500ns, and the remaining pileup for the large detector was about 3% of the detected count-rate.

The DataFurnace computation engine was NDFv9.2b [21]. Errors in the algorithm are mostly in the treatment of the high energy tails of pronounced edges [22]. Moderate layer roughness in a layer structure is calculated through its equivalent excess energy straggling [23-24]. This is not valid for the severe roughness often designed into PV films for maximum light absorption, but IBA spectra from such rough films can also be calculated [25]. NDF has a double scattering calculation [21], and this was included here.

The PIXE data were analyzed using the DATT-PIXE code of Reis [14] as implemented in NDF by the LibCPIXE module [15]. LibCPIXE interprets characteristic X-ray line areas extracted from the raw data using GUPIX [26-27]. We use a manual procedure in this present work, where we apply cross-section corrections obtained by comparison to X-ray yields calculated (for simplified structures) from GUPIX, using its GUYLS utility (which also gives the fluorescence correction: <1% in these structures).

IV. RESULTS

Fig. 1 shows the particle spectra collected with two detectors from an as-deposited CuInAl metallic precursor on Mo/glass. Since the scattering cross-sections of Al are small compared to those of Cu and In, there is no detectable direct Al signal in the RBS spectra, but the Al content of the film significantly affects the spectral shape. The spectra have been fitted with the three-layer structure as shown in Fig. 2, where the first layer has excess In to account for the excess yield in channel 245 (for the large angle detector), and the third layer has no Cu, to account for the spectral dip at channel 166. This dip cannot be fitted unless the second layer has a thickness variation ("roughness") of 11%. The total collected charge is determined through the Mo energy loss by the Mo "substrate" signal. The problem is that the Mo energy loss is not known sufficiently accurately to determine the Al content with any precision. The layers both at the surface and the interface are ambiguously determined in this analysis. To account for the interface signal (at ch.166 for the large detector) we have to introduce an invisible element, but it doesn't have to be Al (as it is in Fig.2): we can also assume that both layers are oxidized.

By themselves the RBS spectra are multiply-ambiguous. How much Al is in the bulk of the CIA film? How much oxidation is happening at the surface and the interface? To identify the Al profile directly we use the (simultaneously collected) He-PIXE spectra, and to get some depth information

from the PIXE data we also collect spectra with the sample tilted normal to the X-ray detector so that the take-off angle is quite different, leading both to very different relative absorptions for the different colour X-rays and also to different ionization cross-sections near the interface.
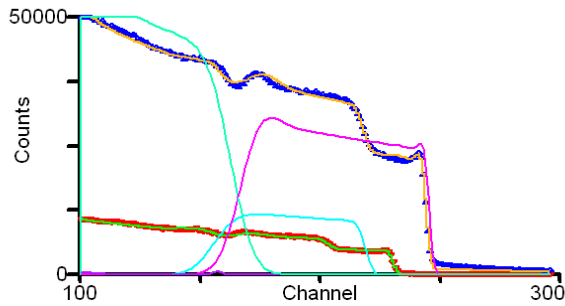

Fig.1. Fitted 1.5MeV He RBS spectra collected simultaneously from two detectors (data – symbols, fits – lines), assuming the 3-layer structure of Fig.2. Partial spectra (calculated before pileup correction) for Mo, Cu, In are shown for the large detector.
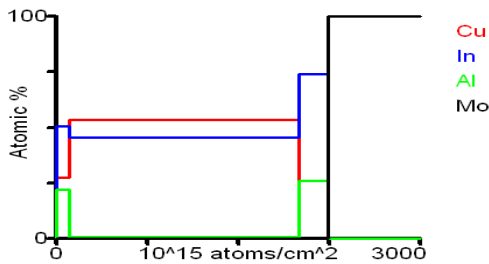

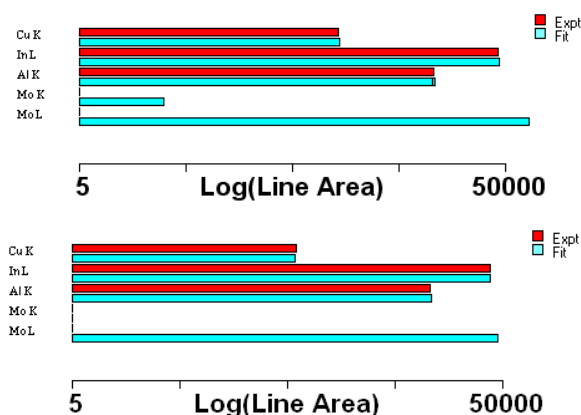*Fig.2. The three layer structure used for fitting RBS spectra of Fig. 1.*

Fig. 3. PIXE line areas and fits from normal beam incidence (above) and normal exit to PIXE detector (below).

By itself, PIXE at two angles only permits distinguishing the front from the back of the CIA film. But the RBS already tells us a great deal about the CIA film, in particular that it is essentially only three layers with excess In at both the surface and the interface. We shall show that the joint RBS/PIXE data gives an unambiguous depth profile of the major and minor elements.

The RBS spectra in Fig. 1 and PIXE data, as shown in Fig. 3, for the sample normal to the beam and normal to the detector, were all self-consistently fitted. Only the characteristic line areas (data and fits) are shown for the PIXE. Theoretical X-ray cross-sections are used [27], except that the In L line cross-section is increased by 22%. Note that both sets of PIXE data are well fitted, consistent at better than 3%, indicating the relative correctness of the solution (including the Al signal) in view of the calculation errors we have listed.
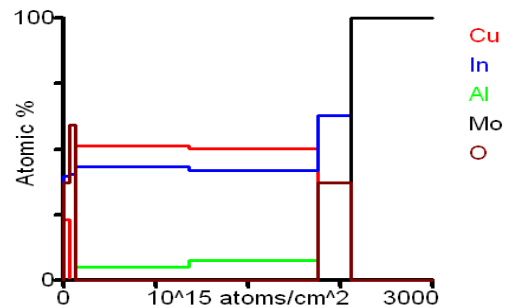

Fig.4. Depth profile extracted from RBS/PIXE data shown in Figs. 1 & 3. Note that the fitting of RBS spectra with this structure model is not shown in Fig.1.

Fig.4 shows the derived depth profile. This has assumed a two-layer structure for the main CIA thin film in which the Al concentration (6.6at% on average) increases towards the interface. It also assumes a two-layer structure for the surface In-rich layer: it is probable that this is an artefact of surface roughness, since the proposed O profile is surprising, and roughness would give the same behaviour with a more plausible profile.

V. CONCLUSIONS

We have demonstrated in a trial manual analysis that CIA metallic precursor films can be unambiguously depth profiled by IBA, except for any Al at the bottom interface of the film. We have shown that an automatic code is available which, with some minor extensions, can readily do an equivalent analysis at the high precision that is usually associ-

ated with these methods, which will allow the Al to be accurately profiled up to the interface.

We have demonstrated both that neither RBS by itself nor PIXE by itself is capable of solving these samples, and also that this can be done by the self-consistent RBS/PIXE analysis that has recently become available.

VII. REFERENCES

[1] I. Repins et al, *Progress in Photovoltaics: Research and Applications,* **16**(2008)235-239.

[2] K. Ramanathan et al, *Proceedings of the 29th IEEE Photovoltaic Specialists Conference*, New Orleans, (2002)523-526.

[3] S. Marsillac et al, *Applied Physics Letters,* **81**(2002)1350-1352

[4] G. Zoppi et al, *MRS Symposium Proceedings,* **1012** (2007)349-354

[5] J. R. Tesmer and M. Nastasi (eds.), *Handbook of Modern Ion Beam Analysis*, Pittsburg: Materials Research Society, 1995

[6] E. Rutherford, *Philosophical Magazine* (Series 6), **21**(1911)669–688

[7] The SRIM (Stopping and Ranges of Ions in Matter) website (2008) http://www.srim.org/

[8] J. F. Ziegler, *Nucl. Instrum. Methods Phys. Res., Sect.* B, **219**(2004)1027-1036

[9] J. F. Ziegler et al, *SRIM - The Stopping and Range of Ions in Matter*, http://www.lulu.com/content/1524197, 2008

[10] K. H. Ecker et al, *Nucl. Instrum. Methods Phys. Res., Sect.* B, **188**(2002)120-125

[11] G. Boudreault et al, *Surf. Interface Anal.*, **33**(2002)478-486

[12] N.P. Barradas et al, *Nucl. Instrum. Methods Phys. Res., Sect.* B, **266**(2008)1338-1342

[13] C. Jeynes et al, *J. Phys. D Appl. Phys.,* **36** (2003)R97-R126

[14] M. A. Reis et al, *Nucl. Instrum. Methods Phys. Res., Sect. B*, **109/110**(1996)134-138

[15] C. Pascual-Izarra et al, *Nucl. Instrum. Methods Phys. Res., Sect. B*, **249**(2006)780-783

[16] C. Pascual-Izarra et al, *Nucl. Instrum. Methods Phys. Res., Sect. B*, **261**(2007)426-429

[17] L. Beck et al, *Nucl. Instrum. Methods Phys. Res., Sect .B,* **266**(2008)1871-1874

[18] J. C. G. Jeynes et al, *Nucl. Instrum. Methods Phys. Res., Sect. B,* **266** (2008)1569-1573

[19] V. Corregidor et al, *Mat. Sci. Forum*, **514-516**(2006)1603-1607

[20] A. Simon et al, *Nucl. Instrum. Methods Phys. Res., Sect. B*, **219-220**(2004)405-409

[21] N. P. Barradas and C. Jeynes, *Nucl. Instrum Methods Phys. Res., Sect. B,* **266**(2008)1875-1879

[22] A. F. Gurbich and C. Jeynes, *Nucl. Instrum. Methods Phys. Res., Sect. B,* **265**(2007)447-452

[23] N. P. Barradas, *J. Phys. D*, **34(14)**(2001)2109-2116

[24] N. P. Barradas, *Nucl. Instrum. Methods Phys. Res., Sect. B,* **190**(2002)247-251

[25] S. L. Molodtsov et al, *J. Phys. D: Appl. Phys.*, **41(20)**(2008)205303

[26] J. Maxwell et al, *Nucl. Instrum. Methods Phys. Res., Sect. B,* **95**(1995)407-421

[27] J. L. Campbell et al, *Nucl. Instrum. Methods Phys. Res., Sect. B,* **170**(2000)193-204